Proceedings of the 43rd "Jaszowiec", International School and Conference on the Physics of Semiconductors, Wisła 2014

Structural and Electronic Properties of Graphene Oxide and Reduced Graphene Oxide Papers Prepared by High Pressure and High Temperature Treatment

M. Tokarczyk[a], G. Kowalski[a], A.M. Witowski[a], R. Koziński[b], K. Librant[b], M. Aksienionek[b], L Lipińska[b] and P. Ciepielewski[b]

[a]Institute of Experimental Physics, Faculty of Physics, University of Warsaw, L. Pasteura 5, 02-093 Warszawa, , Poland

[b]Institute of Electronic Materials Technology, Wólczyńska 133, 01-919 Warszawa, Poland

"Graphene paper" prepared by new proprietary method involving high pressure and high temperature treatment in the reduction process show new possibilities in this area. Different phase content: multilayer and single layer graphene stacks recorded in this study for RGO samples are accompanied by the specific electric and optical parameters. We have found that process temperatures above 900 °C play crucial role in structural and other properties. For the process temperature around 2000 °C we found the onset of the graphitization in the samples.

DOI: 10.12693/APhysPolA.126.1190

PACS: 61.48.Gh, 61.72.Dd, 63.22.Rc

1. Introduction

High performance planar supercapacitors and anodes for new generation lithium ion batteries may both rely on development of new materials based on graphene and graphene oxide. Novel materials based on exfoliated graphene oxide nano-platelets have received increasing attention recently. Solutions of graphene oxide (GO) platelets exfoliated in the combined chemical and mechanical (sonification) processes act as precursors to obtain so called reduced graphene oxide (RGO) papers. Carbon nanotube (CNT) Buckypaper [1–9] and GO paper [10–12] have been already extensively studied even before the onset of "graphene era".

Graphene paper is new, very interesting and perspective material. Self-standing paper-like material built from graphene sheets stacked together, can combine many useful properties like mechanical strength and flexibility [13] with thermal and electrical properties [14].

Stacking sequence and number of layers of nanosheets of graphene present in the paper samples play important role [15, 16] in the electronic and electrochemical properties of the material studied.

Our goal was directed towards development of new proprietary method of obtaining GO and RGO papers [17].

2. Samples

Graphite (Asbury1) was oxidized via Marcano oxidation process [18]. To a mixture of concentrated sulphuric and phosphoric acids graphite flakes were added followed by potassium permanganate. Graphite oxide was purified by sedimentation and centrifugation and exfoliated by sonification process. Recently developed new method [17] of forming the paper sheets was used to obtain GO paper samples and then used subsequently as precursor to obtain RGO papers.

We have chosen for our study two groups of samples of RGO papers reduced by combined thermal and pressure treatment. First series of RGO paper (MPx) consists of four samples which have been annealed at 2000 °C in Ar atmosphere with different Ar pressure (10, 50, 150, and 300 MPa). Second group of RGO/GO papers (Tx) was assembled from another three samples annealed in constant flow (1–1.5 MPa) of N_2 gas but with varying temperature of the process (500 ,750, 900 °C). GO precursor paper was used in this study as reference sample. Both groups were prepared by new proprietary method.

3. Experimental characterization

3.1. SEM

Scanning electron microscopy (SEM) and X-ray diffraction methods were employed for structural studies of the samples. Representative example of SEM cross-sectional images of the samples prepared by standard filtration method and new proprietary method [17] are shown in Fig. 1. It can be easily seen that new method results in more uniformly stacked assembly of macro sheets constituting the GO paper, as seen in all samples manufactured so far by this method. The same was achieved for RGO samples.

3.2. X-ray diffraction

Our X-ray laboratory setup employed Philips X-pert diffractometer which was equipped with a Cu sealed tube X-ray source. Diffractometer was outfitted with a Philips parallel beam Bragg X-ray mirror in front of the X-ray tube. We have used this setup to measure the diffracted intensity around standard angular positions for (002) reflection of graphite and (001) reflection of GO assemblies. We have also directed our attention to the angular position of (10) reflection of 2-dimensional (2D) lattices consisting only of single graphene species (planes)

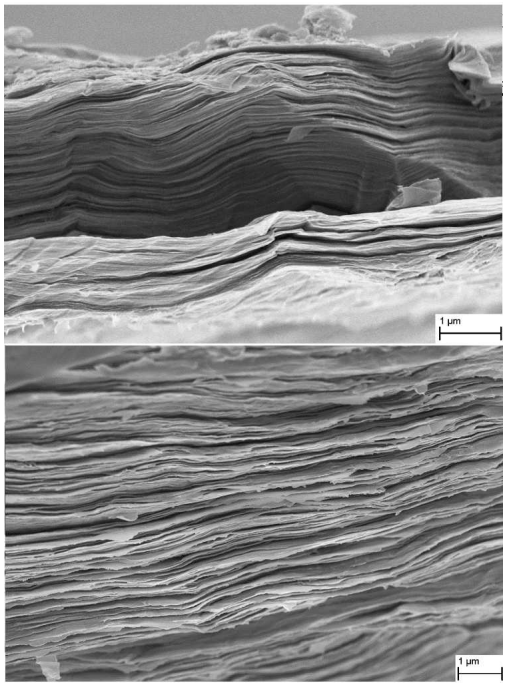

Fig. 1. Example of SEM pictures of graphene oxide paper made by standard filtration method (top) and new proprietary method (bottom). Macro layer structure characteristic for "graphene paper" can be seen in both cases.

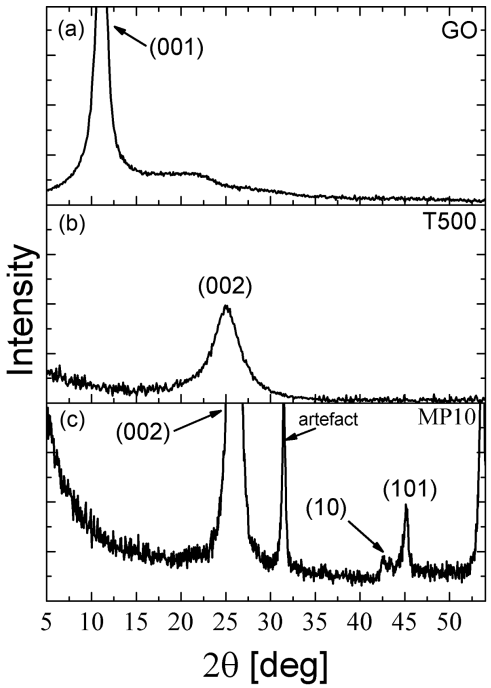

Fig. 2. Examples of full X-ray intensity recorded in θ-2θ scans for (a) GO (precursor) sample, (b) RGO sample T500, (c) RGO sample MP10. Peaks around 26 deg are (002) graphite type reflections. Peak around 11 deg is (001) GO type reflection. Sharp peak on the right hand side of the (002) MP10 sample (bottom curve) is mounting artefact and should be disregarded.

present in the samples. That involves both GO and RGO single 2D platelets since both are built around single graphene lattice. GO samples may basically involve single graphene undisturbed lattice phase only decorated by various "oxide" groups perpendicularly to the main graphene plane.

Our X-ray measurements revealed that the nanosheets of reduced graphene oxide (RGO) have turbostratic stacking arrangement and interplanar spacing above standard graphite value ($d > 3.35$ Å). In the case of graphene oxide (GO) the spacing is typically at least twice larger due to the presence of "oxide" groups intercalating between the graphene planes. Examples of typical diffractometer scans recorded for either GO and RGO samples are shown in Fig. 2. Number of atomic planes in the stack present in the grains of GO and RGO species in the paper were calculated on the basis of standard Scherrer formula or simulated according to the formula in [19, 20].

Recorded scans show unanimously that GO samples show standard position of (001) reflection of GO platelets assembled in multilayer stacks (5–8 planes) with interplanar spacing $d = 7.3$–7.5 Å (Fig. 2a). We have also recorded significant signal at the angular position for (10) 2D reflection from single graphene planes dispersed in the sample (Fig. 3a). Since the position is the same for both GO or RGO lattices we are not specifying which species are present.

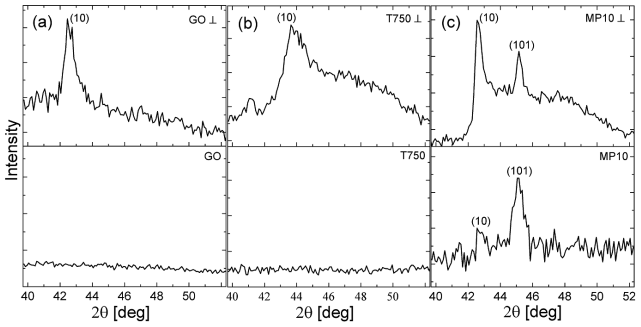

Fig. 3. Examples of X-ray intensity recorded around position for 2D (10) reflection and 3D (101) reflection for two geometrically different positions of the sample with respect to the incoming X-ray beam (positions perpendicular to each other) (a) GO (precursor), (b) RGO T750, (c) RGO MP10.

Generally, we have obtained similar pattern for all RGO samples with the position of the main peak for (002) reflection this time giving the interplanar spacing $d = 3.4$ Å characteristic for graphite type species (Fig. 2b and Fig. 2c). We have again recorded the (10) 2D reflection of the single graphene planes (Fig. 3b and c) bearing in mind that the distinction between "oxide" decorated and pure graphene planes may be unclear. For the samples of MPx series this time (10) 2D reflection is accompanied by standard (101) graphite reflection (Fig. 3c). This means that we do have in our RGO samples

additional phases. RGO MPx sample consists of "bulk" stacked (Turbostratic) assembly of graphene planes with varying number of planes in the stack (30 to 40 on average). This is accompanied by single graphene platelet phase. The presence of the (101) reflection in the spectra for MPx samples (Fig. 3c) indicates that at least some of the "grains" in the sample may be AB stacked which constitutes third phase. For the Tx series of samples we have recorded only two phases: "bulk" turbostratic graphite type phase ((002) peak) and 2D single graphene plane phase ((10) 2D peak). This time bulk phase consists only of few layer stacks (6–8) of graphene planes.

Summary of the main X-ray parameters deduced from the X-ray measurements are assembled in Table I.

TABLE I

Main parameters of the characteristic X-ray lines recorded, with the estimated values of the interplanar d spacing. Number of planes in the stack calculated on the basis of standard Scherrer formula or simulated according to the formula in [19, 20].

Sample	Sample type GO/RGO	Angular peak position 2θ [°]	FWHM [°]	d [Å]	Number of planes in the stack (N)
Precursor	GO	11.182	1.437	7.91	7
T500	RGO/GO	25.065	3.27	3.49	6
T750	RGO/GO	25.848	2.551	3.43	8
T900	RGO/GO	26.17	3.70	3.40	6
MP10	RGO	26.07	0.52	3.418	42
MP50	RGO	26.069	0.52	3.418	42
MP150	RGO	26.047	0.508	3.421	43
MP300	RGO	26.026	0.645	3.424	34

3.3. Raman spectroscopy

Raman spectra were measured with a Renishaw in Via Raman Microscope at 532 nm wavelength (Nd:YAG laser) and low power (0.5 mW; to avoid damage of the sample during measurements).

Raman spectra observed for GO precursor sample (Fig. 4a) are similar to the already observed spectrum for this type of samples [18]. In our case it is accompanied by the significant background signal spread over whole range of the recording. It can be attributed (background) to the luminescence signal already evidenced in this type of samples [21].

Spectra recorded for RGO/GO T500 sample (similar for all Tx type samples in this study) shown in Fig. 4b is very analogous to the precursor spectra as far as intensity of the main peaks is concerned. The only exception is a lack of luminescence background.

Example of the Raman spectrum typically recorded for all MPx type samples (MP10 sample) is shown in Fig. 4c. Basically it shows classic spectrum of the multilayer graphene with D, D', G and $2D$ peaks clearly visible.

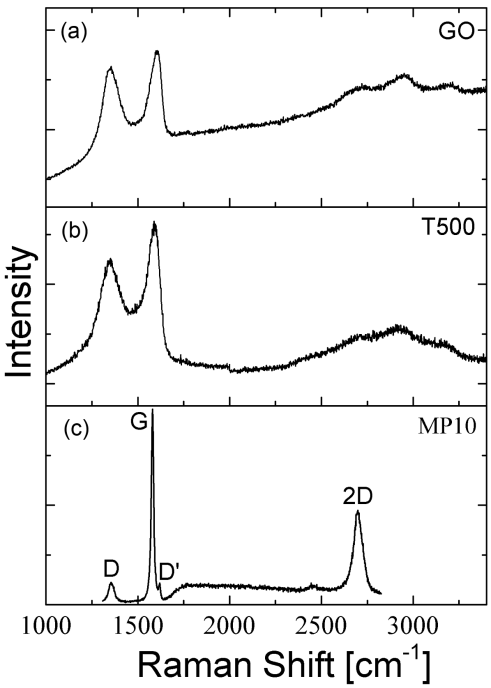

Fig. 4. Examples of Raman spectra recorded for (a) GO precursor, (b) RGO T500 sample, (c) RGO MP10 sample.

3.4. Electrical measurements

Electrical parameters of the samples in this study were characterized by four-point probe and microwave contactless technique to find a paper sheet resistance. The Hall effect in the van der Pauw configuration was measured to establish concentration and mobility of charge carriers in the samples as well as surface resistivity. Measurements are summarised in Table II.

TABLE II

Sheet resistivity, carrier concentration, mobility of RGO/GO and RGO samples.

Sample	Four point probe resistivity [Ω/□]	Hall measurements		
		Carrier concentration [1/cm^2]	Carrier mobility [cm^2/V s]	Resistivity [Ω/□]
T500	128.65	9.89×10^{15}	5.18	121.5
T750	55.7	7.3×10^{17}	0.17	49.59
T900	9.08	5.34×10^{17}	1.23	9.44
MP10	0.99	5.92×10^{15}	1.13×10^{3}	0.931
MP50	0.98	5.42×10^{15}	1.23×10^{3}	0.925
MP150	1.0	5.4×10^{15}	1.15×10^{3}	1.0
MP300	1.14	7.34×10^{15}	0.76×10^{3}	1.11

Resistivity obtained by both methods show very similar results for all samples. Two series of samples (Tx and MPx) show very distinctive difference as far as resistivity is concerned.

All MPx samples have the sheet resistivity around 1 $\Omega/\square$ but Tx samples have the value of resistivity of 1 to 2 orders of magnitude bigger. Carrier mobility is again very much different for both sets of samples. It is shown that temperature (samples Tx) has stronger influence on the resistivity rather than pressure itself (MPx samples).

3.5. Optical characterization

Various groups of oxidising agents present in the GO precursor sample showed their marks in IR spectra (see Fig. 5). Broad peak at about 3200 cm^{-1} indicates presence of carboxyl groups. Line at about 1700 cm^{-1} indicates carbonyl groups. Lines at 1427, 1273, and about 1100 cm^{-1} indicate C–O type bonds. GO also contains aromatic structure since peak about 1600 cm^{-1} indicates C=C double bond.

In the GO precursor papers they are mainly present as intercalate between the graphene planes. It is confirmed by the presence of the (001) diffraction peak shown in Fig. 2.

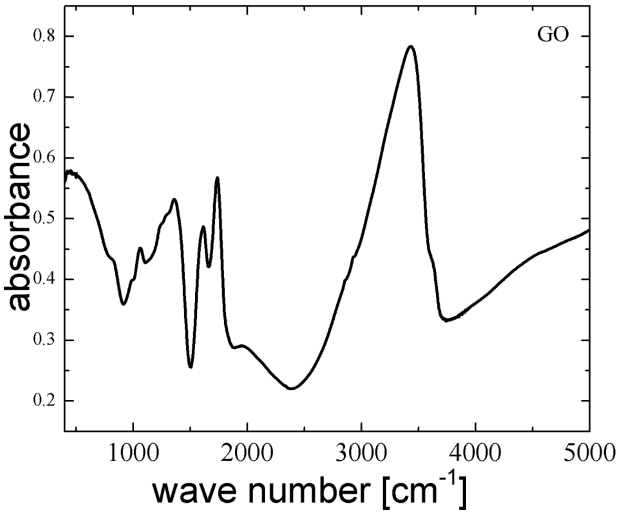

Fig. 5. Absorbance spectra of GO precursor showing the structures due to vibrations in various groups of oxidising agent.

The optical measurements in the infrared and terahertz region for the both groups of samples showed typical plasma behaviour. The "plasma frequency" shows strong sample dependence and may be connected with the percentage of different phases present in the samples. The RGO/GO paper is not transparent, which is probably due to the strong free carrier absorption in the THz region and intense scattering for higher energies. No plasma behaviour was observed for the GO precursor sample.

The reflectivity data were fitted using dynamic dielectric function in the Drude approximation and main results are shown in Table III.

A very tin GO paper allows us to study transmission even in visible region. However the absorbance does not exhibit any trace of interband transitions due to the scattering of light proportional to λ^{-3} .

TABLE III

Drude model parameters to fit the dielectric function.

Sample	Sample type GO/RGO	ω_p [cm^{-1}]	γ [cm^{-1}]	ε_∞
T500	RGO/GO	235	310	1.7
T750	RGO/GO	265	320	1.7
T900	RGO/GO	170	160	0.9
MP10	RGO	205	231	4.6
MP50	RGO	242	216	4.7
MP150	RGO	544	126	3.4
MP300	RGO	265	335	2.6

4. Discussion and conclusions

Our structural studies have shown that the samples examined in this study show at least 2 to 3 phases present in the volume of the material.

- GO precursor: turbostratic intercalated by "oxy" groups graphite phase ($d = 7.9$ Å, $N = 7$) and single graphene 2D phase (decorated by "oxy" groups);
- Tx samples: turbostratic graphite-like phase ($d = 3.4$ Å, $N = 6-7$), single graphene 2D phase (probably still decorated by "oxy" groups to some extent);
- MPx samples: turbostratic graphite-like phase ($d = 3.4$ Å, $N = 30-40$), single graphene 2D phase, graphite like (AB) 3D phase. Partially graphitized sample.

The Raman and X-ray studies indicate that graphitization process already started. Both series of samples show macroscopic assembly of the planar but slightly corrugated macrosheets (Fig. 1, SEM). Electrical measurements show very distinct resistivity and mobility differences between two series of the samples. They can be attributed to the structural differences found in the samples resulting from the temperature and pressure treatment.

Strong similarity between the Raman spectra for GO precursor and Tx series show that in this type of RGO/GO material simple distinction (between pure GO and RGO) based only on the Raman measurements is not possible. Possible explanation for this resemblance may lay in the similarities in the structure (two phases) and the presence of the oxidising groups still attached to the 2D phase (single graphene decorated by the "oxy" groups). Probably the temperatures used in the reduction process were to low to fully remove "oxy" groups from the material. Full reduction was achieved for the 2000 °C as for MPx samples. Our study show that reduction process of the GO precursor involving varying the temperature and accompanying gas pressure may be crucial in achieving the required parameters

(structural and electrical) as specified for particular applications of the final nanostructured material.

Tunable microstructure and resulting resistivity, carrier mobility and optical parameters of the paper via high P/high T treatment may be the way to further development of the material according to the specific application requirements.

Acknowledgments

This work was supported by GRAFTECH/NCBR/02/19/2012 "FLOWGRAF".

References

[1] S.M. Cooper, H.F. Chuang, M. Cinke, B.A. Cruden, M. Meyyappan, *Nano Lett.* **3**, 189 (2003).

[2] Z. Wang, Z. Liang, B. Wang, C. Zhang, L. Kramer, *Composites Part A* **35**, 1225 (2004).

[3] M. Endo, H. Muramatsu, T. Hayashi, Y.A. Kim, M. Terrones, M.S. Dresselhaus, *Nature* **433**, 476 (2005).

[4] P. Gonnet, Z. Liang, E.S. Choi, R.S. Kadambala, C. Zhang, J.S. Brooks, B. Wang, L. Kramer, *Curr. Appl. Phys.* **6**, 119 (2006).

[5] J. Gou, *Polym. Int.* **55**, 1283 (2006).

[6] Y.A. Kim, H. Muramatsu, T. Hayashi, M. Endo, M. Terrones, M.S. Dresselhaus, *Chem. Vap. Deposit.* **12**, 327 (2006).

[7] F. Zheng, D.L. Baldwin, L.S. Fifield, N.C. Anheier, C.L. Aardahl, J.W. Grate, *Anal. Chem.* **78**, 2442 (2006).

[8] D. Wang, P. Song, C.L. Liu, W. Wu, S. Fan, *Nanotechnology* **19**, 075609 (2008).

[9] G. Xu, Q. Zhang, W. Zhou, J. Huang, F. Wei, *Appl. Phys. A Mater. Sci. Process.* **92**, 531 (2008).

[10] D.A. Dikin, S. Stankovich, E.J. Zimney, R.D. Piner, G.H.B. Dommett, G. Evmenenko, S.T. Nguyen, R.S. Ruoff, *Nature* **448**, 457 (2007).

[11] H. Chen, M.B. Muller, K.J. Gilmore, G.G. Wallace, D. Li, *Adv. Mater.* **20**, 3557 (2008).

[12] S. Park, K. Lee, G. Bozoklu, W. Cai, S.T. Nguyen, R.S. Ruoff, *ACS Nano* **2**, 572 (2008).

[13] A.R. Ranjbartoreh, B. Wang, X. Shen, G. Wang, *J. Appl. Phys.* **109**, 014306 (2011).

[14] H. Wu, L.T. Drzal, *Carbon* **50**, 1135 (2012).

[15] X. Yang, J. Zhu, L. Qiu, D. Li, *Adv. Mater.* **23**, 2833 (2011).

[16] Y. Hu, X. Li, D. Geng, M. Cai, R. Li, X. Sun, *Electrochim. Acta* **91**, 227 (2013).

[17] R. Kozinski, K. Librant, M. Aksienionek, Z. Wiliński, L. Lipińska, *Abstracts of GRAPHEsp2014, Lanzarote (Spain)*, 2014, unpublished results.

[18] D.C. Marcano, D.V. Kosynkin, J.M. Berlin, A. Sinitskii, Z. Sun, A. Slesarev, L.B. Alemany, W. Lu, J.M. Tour, *ACS Nano* **4**, 4806 (2010).

[19] M. Tokarczyk, G. Kowalski, M. Możdżonek, J. Borysiuk, R. Stępniewski, W. Strupiński, P. Ciepielewski, J.M. Baranowski, *Appl. Phys. Lett.* **103**, 241915 (2013).

[20] M. Tokarczyk, G. Kowalski, K. Grodecki, J. Urban, W. Strupiński, *Acta Phys. Pol. A* **124**, 768 (2013).

[21] Z. Luo, P.M. Vora, E.J. Mele, A.T. Charlie Johnson, J.M. Kikkawa, *Appl. Phys. Lett.* **94**, 111909 (2009).